Rheology of concentrated dispersions of sterically stabilized polydisperse lamellar droplets

Kevelam, J; Hoffmann, A.C; Engberts, J.B.F.N.; Blokzijl, W.; van de Pas, J.C.; Versluis, P.

Published in:
Langmuir

DOI:
10.1021/la9816353

Publication date:
1999

Rheology of Concentrated Dispersions of Sterically Stabilized Polydisperse Lamellar Droplets

Jan Kevelam, Alex C. Hoffmann, and Jan B. F. N. Engberts*

Stratingh Institute, University of Groningen, Nijenborgh 4, 9747 AG Groningen, The Netherlands

Wilfried Blokzijl, John van de Pas, and Peter Versluis

Unilever Research Vlaardingen, Olivier van Noortlaan 120, 3133 AT Vlaardingen, The Netherlands

Received November 23, 1998. In Final Form: April 26, 1999

The rheological behavior of concentrated dispersions of sterically stabilized lamellar droplets has been studied as a function of the molecular weight and of the amount of adsorbed hydrophobically endcapped poly(sodium acrylate)s. The chemical compositions of the samples are identical to those described before. Despite the polydispersity of the sample, scaling laws and equations that are well established in the rheology of monodisperse colloidal suspensions can be successfully applied. Although the amount of added stabilizing polymer at constant molecular weight hardly influences the elastic modulus (G') as a function of (core) volume fraction of lamellar droplets (ϕ_{lam}), increasing the polymer molecular weight at constant grafting density results in a pronounced increase of the elastic modulus. The ratio of particle radius to adsorbed layer thickness (R/Δ) decreases with molecular weight, thereby increasing the effective volume fraction. A peculiar effect occurs if the polymer molecular weight drops below 1000. Polymer molecules penetrate into the lamellar droplets, and ϕ_{lam} is increased (at constant surfactant concentration). This so-called "building-in" effect can be used to thicken lamellar dispersions. Thickening can also be induced by addition of "bridging polymers", which carry multiple hydrophobic anchors, linking several droplets. Concomitant adverse effects of bridging flocculation can be counteracted by admixing of hydrophobically endcapped polymers; the resulting dispersions are characterized by enhanced shear-thinning behavior and good physical stability.

Introduction

Control of the rheological properties of colloidal dispersions is of great industrial importance, both during processing and for end-product properties. Shear-thinning behavior is often desirable, providing the dispersion with a low viscosity when sheared (i.e., in milling, stirring, or even pouring), whereas at rest, the system has a certain solidlike consistency.

We will focus on the rheological properties of sterically stabilized multilamellar vesicles composed of anionic and nonionic surfactants, dispersed in a concentrated aqueous electrolyte solution.[1] A balance of attractive, repulsive and "randomizing" Brownian forces determines the overall rheological characteristics of the dispersion. The attractive forces are due to osmotic attractions between salted-out nonionic headgroups (vide infra) and, less importantly, to van der Waals interactions. On the outside of the particles, a polymer is adsorbed through anchoring of its hydrophobic side-chains into the vesicle bilayers. The dispersing medium is a "good" solvent for the polymer backbone; hence, the adsorbed layer introduces a repulsive "steric" force that is osmotic in nature.[2]

In this paper, only concentrated dispersions will be described, where the volume fraction of lamellar droplets (ϕ_{lam}) exceeds 0.5. In the volume fraction regime $\phi_{lam} > \sim 0.8$, particle−particle interactions dominate through overlap of repulsive layers. A so-called repulsive network of colloidal particles is formed, which has not only liquidlike (viscous) but also elastic properties. The application of a small mechanical force causes a small deformation of the system and a consequent distortion of the interparticle arrangement. Deviations from the equilibrium interparticle distance result in a potential energy increase, and the particles react by exerting an opposing force. This is the origin of the elastic response of the network. Thus, in principle, the bulk rheological properties of a system, and in particular its elastic modulus (G'), can be predicted from the interparticle pair potential and vice versa, and this has been the holy grail in experimental and theoretical rheology since the pioneering work of Buscall et al.[3] It is not surprising that in this ongoing quest well-defined model systems have been studied, using monodisperse (latex or silica) particles of accurately known size, stabilized by electrostatic forces or with the use of monodisperse polymers grafted at any desired surface occupancy and at well-known adsorbed layer thicknesses.

These studies have yielded many important insights into the relationships between dispersion microstructure and bulk rheological properties, and the aim of this study is to apply the obtained insights to the rheological investigation of a much more complex system, where the particle size is polydisperse, and in which case added polymer not just increases the grafting density but also decreases the average particle size. The microstructural features of the lamellar dispersion, as a function of both polymer concentration and molecular weight, have been described before,[4] and serve as a starting point for the present rheological investigation. Thus, we will investigate

(1) Van de Pas, J. C. Ph.D. Thesis, University of Groningen; Groningen, The Netherlands, 1993.

(2) Hesselink, F. Th.; Vrij, A.; Overbeek, J. Th. G. *J. Phys. Chem.* **1971**, *75*, 2094.

(3) Buscall, R.; Goodwin, J. W.; Hawkins, M. W.; Ottewill, R. H. *J. Chem. Soc., Faraday Trans. 1* **1982**, *78*, 78.

10.1021/la9816353 CCC: $18.00
Published on Web 06/19/1999

Scheme 1

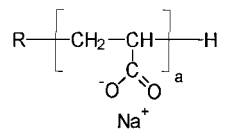

EC750 - EC34000: a = 6-370
R = $C_{11}H_{23}[CO_2]$ or $C_{12}H_{25}S$

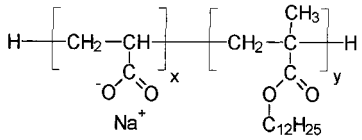

HMNAR: x/y = 18/1, M_n = 21,000

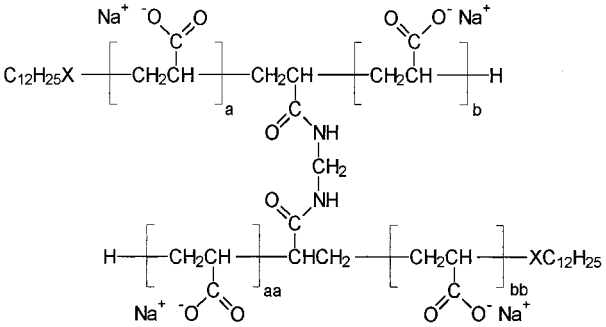

CL3500 / CL9000:
Average mol. wt. of hydrophilic chains (a+b), (aa+bb), ... = 3500 / 9000.

lamellar dispersions with added hydrophobically end-capped poly(sodium acrylate)s having a molecular weight ranging between 750 and 30 000.

Another aim is to study even more complicated cases where the polymer not only anchors into the outer bilayer of the lamellar droplet but penetrates the multilamellar aggregates to reside in the water layers. This phenomenon of "building-in" will be explored in some detail, with regard to consequences for microstructural and rheological properties of the dispersion.

Finally, interesting structuring phenomena arise when polymers carrying multiple hydrophobic anchors are added to the dispersion. Provided that these so-called "bridging polymers" remain largely at the surface of the droplets, they can hydrophobically link two adjacent droplets. As a consequence, bridging flocculation might occur, and it is of interest to investigate the influence of bridging polymers on the physical and colloidal stability of the dispersions. A more practical question that we wanted to answer is whether shear-thinning behavior of sterically stabilized dispersions can be enhanced by admixing bridging polymers, in such a way that the dispersion is endowed with particle suspending power while at the same time remaining sufficiently pourable.

Experimental Section

Materials. *1. Hydrophobically Single-Endcapped Stabilizing Polymers.* The synthesis and characterization of the hydrophobically single-endcapped stabilizing poly(sodium acrylate)s (Scheme 1) have been described before.[4] The chemical structures of the polymers have been abbreviated for clarity. As an example, EC750 refers to a hydrophobically endcapped poly(sodium acrylate) of molecular weight 750.

2. Synthesis and Characterization of Bridging Polymers. A bridging polymer containing hydrophobic anchors distributed randomly along the sodium acrylate backbone, HMNAR, was synthesized by radical polymerization of 19.5 g (271 mmol) of freshly distilled acrylic acid (Acros, 99%) and 2.75 g (10.8 mmol) of lauryl methacrylate (Aldrich, 96%) in 200 mL of 1,4-dioxane (Merck, p.a.) in the presence of 0.19 g (0.23 mmol) of dilauroyl peroxide as an initiator. The mixture was kept under a nitrogen atmosphere at 80 °C for 12 h. After cooling to room temperature, the clear, slightly viscous solution was precipitated in 1 L of pentane to remove most of the 1,4-dioxane. The viscous precipitate was dissolved in dry methanol. The methanolic solution was slowly added to a stirred solution of 14 g (260 mmol) of sodium methoxide (Merck) in 400 mL of dry methanol. A white solid precipitated, which was filtered off under reduced pressure. The crude product was dried in vacuo at 30 °C to remove most of the remaining 1,4-dioxane and methanol. The polymer was dissolved in water to obtain a solution of about 5−10% (w/w). The polymer was neutralized by adding sodium hydroxide until pH 9, and the solution was freeze-dried. To remove the last traces of solvent, the polymer was finely powdered and dried at 60 °C over P_2O_5 in vacuo for at least 2 h. The isolated yield was 77%. By ^{1}H NMR spectroscopy, the ratio of lauryl methacrylic to acrylic monomeric units in the polymer was determined as 1:18. Molecular weight characteristics of HMNAR are presented in Table 1.

Table 1. Molecular Weights of Hydrophobically Modified Poly(sodium acrylate)s as Determined by NMR and Size Exclusion Chromatography (SEC)

polymer	M_w (SEC)	M_n (SEC)	M_n (NMR)	M_w/M_n (SEC)
EC750	605	360	750	1.8
EC1500	2 700	1 900	1 500	1.4
EC3000	4 300	3 100	3 000	1.4
EC8500	25 000	10 000	8 500	2.5
EC29000	82 000	27 000	29 000	3.0
CL3500	82 000	19 000	n.a.	4.3
CL9000	41 000	12 000	n.a.	3.4
HMNAR	26 000	21 000	n.a.	1.2

Two bridging polymers were obtained by cross-linking of hydrophobically endcapped poly(sodium acrylate)s, using *N*,*N*′-methylenebisacrylamide as a cross-linking agent. A polymer with a kinetic chain length of 36 acrylate units was synthesized as follows. A 250 mL round-bottomed flask was loaded with 5 g (69.4 mmol) of freshly distilled acrylic acid (Acros, 99%), 0.011 g (0.069 mmol) of *N*,*N*′-methylenebisacrylamide (Aldrich, 99%), 50 mL of 1,4-dioxane (Merck, pro analysi), 0.5 g (1.5 mmol) of *n*-dodecyl thiol, and 0.6 g (1.50 mmol) of dilauroyl peroxide (Aldrich). The flask was connected to a reflux condenser fitted with a $CaCl_2$ tube and was heated on an oil bath at 80 °C with stirring. The reaction mixture was kept at this temperature overnight. During the reaction, the polymer precipitated as a white solid. After cooling to room temperature, the solid was dissolved in 50 mL of methanol and subsequently precipitated in 300 mL of pentane to remove most of the 1,4-dioxane. The

(4) Kevelam, J.; Martinucci, S.; Engberts, J. B. F. N.; Blokzijl, W.; Pas, J. C. van de; Blonk, J. C. G.; Versluis, P.; Visser, A. W. J. G. *Langmuir* **1999**, *15*, 4989.

viscous precipitate was dissolved in dry methanol. The methanolic solution was slowly added to a stirred solution of 3.6 g (66.7 mmol) of sodium methoxide (Merck) in 100 mL of dry methanol. A white solid precipitated, which was filtered off under reduced pressure. The crude product was worked up as described above. Another polymer, with a kinetic chain length of 96 acrylic units, was synthesized analogously but in the absence of *n*-dodecyl thiol.

As mentioned above, the cross-linked polymers have number-averaged kinetic chain lengths of 36 and 96 (as determined by ^{1}H NMR spectroscopy) and are denoted as CL3500 and CL9000, respectively. Number- and weight-averaged molecular weights were determined using size exclusion chromatography and are summarized in Table 1.

3. Lamellar Dispersions. The preparation of 40/60/20-type dispersions of lamellar droplets has been described before.[4] Briefly, 28 weight parts of sodium dodecylbenzene sulfonate and 12 weight parts of nonionic surfactant Synperonic A7 ($C_{13-15}EO_{\langle 7\rangle}$) are added to an aqueous premix containing 20 weight parts of trisodium citrate and 60 parts of water. A dispersion of multilamellar vesicles (instead of a micellar solution) is formed because the surfactants are salted-out. As a result, attractive osmotic forces between nonionic surfactant headgroups dominate, and the lamellar droplets flocculate. Phase separation occurs to form a surfactant-rich phase where the volume fraction of lamellar droplets ($\phi_{\rm lam}$) is unity, and an aqueous electrolyte solution contains no surfactants at all. By separating the phase and remixing in different proportions, lamellar dispersions of any desired $\phi_{\rm lam}$ can be obtained.

In $\phi_{\rm lam}$-dependent studies, stabilizing polymers of different molecular weight have been added to obtain a constant ratio of hydrophobic anchors to surfactant molecules. A 40/60/20 model system containing 1% (w/w) of EC7800 has been chosen as a reference. As an example, a more concentrated sample with 60 wt % of surfactants contains (60/33.33) × 1% = 1.8 wt % of EC7800.

Methods. *1. Oscillatory Rheometry.* Most rheological measurements were performed at 25.0 °C using a Bohlin VOR rheometer in oscillatory mode. Herein, a sinusoidally varying strain of known amplitude is applied, and the resulting sinusoidal stress is measured. Generally, the stress will be shifted out of phase due to the viscoelastic properties of the sample. The in-phase component of the complex modulus (G^*) is the elastic response (G'), whereas the 90 degrees phase-shifted component reflects the viscous behavior of the sample (G''). Some intuition for the physical significance of the moduli can be obtained by imagining what happens when pulling an elastic: the Hookean (springlike) response is immediate (in-phase), and the expression of its fluidlike character is lagging behind. Before carrying out each measurement of G^* as a function of frequency ($10^{-3} < \nu < 10^1$), a strain sweep was performed, where the applied strain (γ) was gradually increased from 0 to 10% at a constant frequency of 1 Hz. The elastic modulus was found to be strain-independent up to $\gamma = 4\%$ and to decrease with increasing strain. Therefore, measurements were carried out below this critical strain ($\gamma_0 = 4\%$), in the linear viscoelastic region, so that the structure of the sample was not perturbed. Importantly, the amplitude was not increased beyond 50% during a strain sweep, to prevent severe perturbation of the structure of the sample. Moreover, the dispersion was introduced carefully into the geometry, using wide-bore pipets without narrow ends (diameter = 1 cm), to prevent excessive shearing.

A concentric cylinder geometry was used with a moving cup of radius 27.5 mm, and a fixed bob (radius = 25 mm). The deflection of the bob due to the sample stress was measured either using torsion bars or by employing an electronic device (low torque head). Both systems, fitted to two different (VOR) rheometers, yielded the same results within 5%.

Concentrated dispersions of sterically stabilized lamellar droplets were equilibrated for at least one week, as recommended before.[3] If necessary, entrapped air bubbles were removed by mild centrifugation prior to the measurements, at ca. 4 000 g, using an AHT 5200 centrifuge.

2. Shear Viscosimetry. Viscosities as functions of shear rate were determined using a Bohlin CS rheometer, equipped with a serrated concentric cylinder setup (bob diameter = 25 mm, gap = 0.125 mm, and grooves = 0.1 mm).[5] Sample handling was as described for the dynamic oscillatory measurements.

3. Light Microscopy. Samples of lamellar dispersions were inspected with a Zeiss Axioplan light microscope, using polarized light, at 10X and 40X magnifications. A small drop of material was placed on a microscope slide and quickly covered with a cover glass. Initially the sample flows to fill the gap between the slide and the cover glass; images were recorded after a few minutes, when the flow had almost stopped.

4. Particle Sizing. Particle sizes were measured by laser diffraction, using a Malvern MasterSizer X long bed, or indirectly determined by colloidal refractometry, as described in Buscall.[3]

5. Electrical Conductivity and Calculation of ϕ_{lam}. The volume fraction of the lamellar phase ($\phi_{\rm lam}$) was calculated from the electrical conductivity of the lamellar dispersion using the Bruggeman equation:[6]

$$\frac{\kappa - \kappa_{\rm lam}}{\kappa_{\rm el} - \kappa_{\rm lam}}\left(\frac{\kappa_{\rm el}}{\kappa}\right)^{1/3} = 1 - \phi_{\rm lam} \qquad (1)$$

where κ denotes the electrical conductivity of the dispersion, $\kappa_{\rm lam}$ is the electrical conductivity of the lamellar droplets and $\kappa_{\rm el}$ refers to the electrical conductivity of the continuous electrolyte phase. Since the employed endcapped poly(sodium acrylate)s contribute much more to the conductivity of the dispersion than the lamellar droplets to which they are adsorbed,[7] measured volume fractions do not include the adsorbed layer thickness.

Electrical conductivity was measured using a Wayne-Kerr Autobalance Universal Bridge B642 fitted with a Philips PW9512/01 conductivity cell having a cell constant of 0.67 cm^{-1}. If necessary, entrapped air bubbles were first removed by mild centrifugation. $\kappa_{\rm lam}$ was found to be 0.7 mS cm^{-1}, which compares favorably with the literature value[8] of 0.8 ± 0.2 mS cm^{-1}; $\kappa_{\rm el}$ = 61 mS cm^{-1}.

6. X-ray Diffraction. Bilayer repeat distances in lamellar droplets were evaluated from X-ray diffractograms. A Kratky small-angle camera, equipped with a Braun PSD counter, was installed on a PW1729 generator with a copper anode (Cu Kα radiation) operated at 2 kW (50 kV, 40 mA).

7. Size Exclusion Chromatography. Polymer molecular weights were determined by size exclusion chromatography. Polymer separation was performed using a sequential array of three columns (Biogel SEC 40XL, 30XL, and 20XL). The fractions were analyzed employing a Viscotek model 200 differential refractive index detector (to determine $M_{\rm n}$) and a tri-angle laser light scattering detector (to determine $M_{\rm w}$).[9]

Results and Discussion

Particle Size Polydispersity and the Maximum Packing Fraction $\phi_{\rm max}$. The sterically stabilized lamellar droplets under study are characterized by a wide size distribution.[4] Typically, the smallest droplets have a diameter of 10^{-2} μm, whereas the largest droplets have a size of 10 μm. Although for monodisperse suspensions the maximum packing fraction of the particles ($\phi_{\rm max}$) is 0.63 (at rest) or 0.71 (under shear),[10] in the system under study, size polydispersity and particle deformability theoretically allow $\phi_{\rm max}$ to reach unity. The rationale is that the small droplets can fill the holes between the large particles; hence, virtually all empty space can be occupied.

(5) Grooving aids in preventing wall slip; see: Jurgens, A. *Tenside Surfactants Deterg.* **1989**, *26*, 222.

(6) Bruggeman, D. A. G. *Ann. Phys.* **1935**, *24*, 636.

(7) As we have measured, small amounts of added polymer even enhance the conductivity of the continuous phase (containing 30% (w/w) sodium citrate), whereas the presence of lamellar droplets in the system lowers the conductivity of the dispersion. The latter effect lies at the heart of the conductometric determination of $\phi_{\rm lam}$.

(8) Van de Pas, J. C. *Tenside Surfactants Det.* **1991**, *28*, 158.

(9) For basic principles, see: Brandrup, J.; Immergut, E. H. *Polymer Handbook*; 3rd ed.; Wiley: New York, 1989.

(10) De Kruif, C. G.; Van Iersel, E. M. F.; Vrij, A.; Russel, W. B. *J. Chem. Phys.* **1985**, *83*, 717.

Figure 1. Freeze-fracture-etching electron micrograph of a 40/60/20-type lamellar dispersion with added EC3000 stabilizing polymer. $\Phi_{lam} = 0.91$ (from conductivity experiments); note that only a little free space (=continuous phase) can be observed between the droplets and how this can be achieved by filling the holes between large droplets with smaller particles. Bar represents 1 μm.

This expectation was confirmed by experimental evidence. By conductometry, the volume fractions of "bare" particles in the most concentrated dispersions were determined as 0.9−0.95, with the remainder of the dispersion volume being occupied by the adsorbed polymer molecules. Freeze-fracture−etching electron micrographs visually support these measurements (Figure 1).

In addition, loss moduli (measured at $\nu = 1$ Hz) were converted into shear viscosities (η) using the Cox-Merz rule[11] for polymeric solutions: $\eta = G''/\omega$, where $\omega = \nu/2\pi$. Although this approach is valid strictly only in the limit that $\omega \rightarrow 0$, it appears that, at least for 40/60/20-type lamellar dispersions with added EC7800 polymer, the experimentally determined steady-shear viscosity correlates surprisingly well with η computed from G''. Moreover, it appears that the steady-shear viscosities (calculated from G'') as a function of volume fraction can be superimposed for all polymer concentrations and that the results can be fitted to the Krieger−Dougherty equation:

$$\frac{\eta_\infty}{\eta_c} = \left(1 - \frac{\phi}{\phi_{max}}\right)^{-[\eta]\phi_{max}} \qquad (2)$$

where η_∞ is the high shear plateau viscosity,[12] η_c is the viscosity of the continuous phase (=3.89 mPa s), and $[\eta] = 2.5$, which is the value predicted for (monodisperse) hard spheres.[12] The fit of eq 2 to the data, using $\phi_{max} = 1$, is shown in Figure 2; the relative viscosity refers to the ratio of η_∞ to η_c.

Frequency Spectra and the Critical Packing Fraction. Plots of G' versus ν as a function of volume fraction all follow the same general trend; that is, G' is virtually frequency-independent at high volume fractions, whereas below a critical packing fraction, G' decreases with decreasing frequency. As an example, we present G' versus $\nu(\phi_{lam})$ maps for two polymers of different molecular weight (Figure 3).

The data can be interpreted as follows. At low volume fractions, the overlap of repulsive layers is small, and at low frequencies, the suspension dissipates energy through particle diffusion rather than by storing energy in particle−particle interactions. When the frequency is increased, the elastic modulus increases because the oscillation is faster than some of the diffusive modes of dissipation. This behavior characterizes liquidlike microstructure (for a true Maxwellian liquid ($\partial \log G'/\partial \log \nu =$ 2). At high ϕ_{lam}, interparticle interactions between adsorbed polymers are strong and numerous, hindering particle self-diffusion. The behavior of the dispersion is typical of that of a viscoelastic solid. The oscillation time is much faster than all diffusive relaxational processes, leaving the storage modulus independent of frequency.[13]

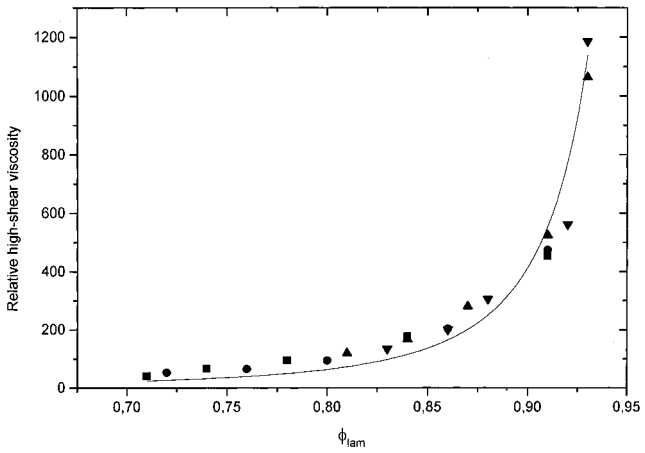

Figure 2. Krieger−Dougherty equation applied to 40/60/20-type lamellar dispersions containing different concentrations of EC7800. High-shear viscosities were calculated from viscous moduli at 1 Hz, employing the Cox−Merz analogy. ■ 0.52 wt %; ● 0.61 wt %; ▲ 1.53 wt %; ▼ 1.77 wt %.

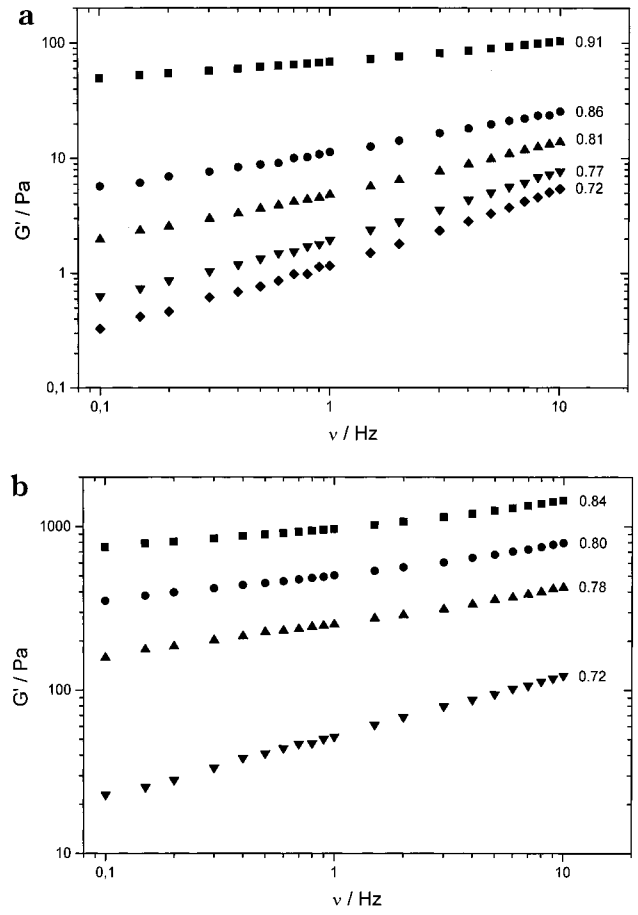

Figure 3. Plots of elastic modulus (G') vs frequency (ν) as a function of ϕ_{lam} for lamellar dispersions with stabilizing polymers of varying molecular weight: EC1000 (A) and EC19000 (B). The numbers to the right of the curves indicate volume fractions. Note that for the higher molecular weight polymer, the slope $\partial \log G'/\partial \log \nu$ starts to decrease at a lower volume fraction (ϕ_{cr}), as mentioned in the text. Moreover, at equal ϕ_{lam}, G' is larger for EC19000 than for EC1000.

(11) Cox, W. P.; Merz, E. H. *J. Polym. Sci.* **1958**, *28*, 619.
(12) Krieger, I. M. *Adv. Colloid Interface Sci.* **1972**, *3*, 111.

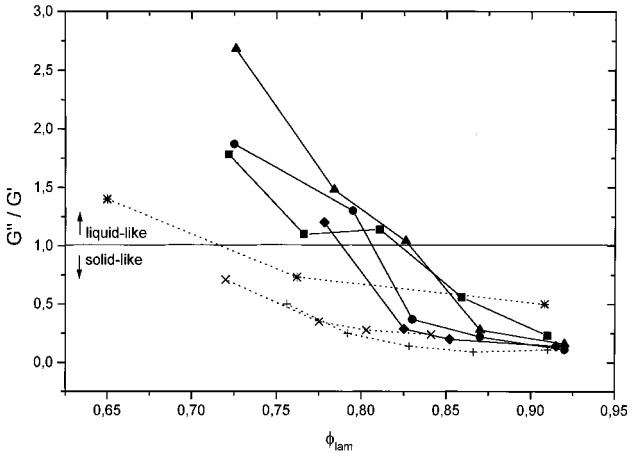

Figure 4. Plots of G''/G' vs ϕ_{lam} as a function of polymer molecular weight. The critical packing fraction is obtained at the volume fraction where $G''/G' = 1$. ▲ EC3000; ● RAN4000; ■ EC1000; ◆ EC5300; ∗ EC34000; + EC7800; × EC19000.

The transition from liquidlike to solidlike behavior occurs at a critical volume fraction (ϕ_{cr}), where the mean particle separation becomes comparable to twice the layer thickness of adsorbed polymer, that is, when the repulsive layers of anchored polymers are just touching. The latter implies that ϕ_{cr} will decrease with increasing polymer molecular weight, due to an increase of the adsorbed layer thickness with respect to the droplet size. This is illustrated in Figure 3.

ϕ_{cr} can also be obtained as the volume fraction when the elastic modulus equals the viscous modulus. The idea is that liquid- and solidlike behavior balance each other at the volume fraction of lamellar droplets where $G' = G''$.[14] Figure 4 demonstrates the approach. As expected, ϕ_{cr} decreases with increasing polymer weight.

Adsorbed Layer Thickness and Polymer Molecular Weight. As was discussed above, ϕ_{cr} is the point where the repulsive layers of adsorbed polymers just start to overlap. Knowledge of ϕ_{cr} therefore enables us to calculate the mean adsorbed layer thickness, provided that the droplet radius (R) is known:

$$\Delta = R\cdot\left[\left(\frac{\phi_{max}}{\phi_{cr}}\right)^{1/3} - 1\right] \qquad (3)$$

Equation 3 has been thoroughly derived for the case of dispersions of monodisperse particles, and the values determined for Δ closely match those obtained using dynamic light scattering.[11,15] However, at the outset, it was not clear whether eq 3 is applicable to dispersions of polydisperse lamellar droplets. For example, there exists no single particle radius, and if substitution of R for an "average" particle radius were valid, one would soon encounter severe problems in trying to define an appropriate mean. We have recently shown that an "average" adsorbed layer thickness can be obtained from the surface-averaged particle radius d[3,2]:[16]

$$\Delta = \mathrm{d[3,2]}\left[\left(\frac{\phi_{max}}{\phi_{cr}}\right)^{1/3} - 1\right] \qquad (4)$$

Table 2. Critical Packing Fractions (ϕ_{cr}) and Adsorbed Layer Thickness (Δ) of Lamellar Droplets with Added Hydrophobically Endcapped Stabilizing Polymers Having Different Molecular Weights

polymer	ϕ_{cr}	d[3,2] (μm[a])	d[1,0] (μm[a])	$\Delta^{[3,2]}$ (nm)	$\Delta^{[1,0]}$ (nm)	R/Δ
EC1000	0.82	4.05	0.77	136	26	30
EC3000	0.83	4.41	0.81	142	26	31
RAN4000	0.81	4.01	0.87	149	32	27
EC5300	0.79	3.65	0.74	151	31	24
EC7800	0.70	2.83	0.33	178	21	16
EC19000	0.68	1.88	0.30	129	21	15
EC34000	0.72	1.49	0.29	88	17	17
CL3500	0.83	3.97	0.95	127	30	31
CL9000	0.70	3.36	0.83	212	52	16

[a] Particle sizes have been determined using laser diffraction (Malvern Mastersizer).[3]

The results obtained are summarized in Table 2. It appears that absolute values of reported adsorbed layer thicknesses are too high. For example, the length of a fully extended poly(sodium acrylate) molecule with a molecular weight of 1000 (ca. 10 acrylate units) is 15 nm at maximum, whereas the measured adsorbed layer thickness is 136 nm. The discrepancy is too large to be accounted for by electrostatic (repulsion) or hydration effects. We contend that experimental difficulties lie at the heart of the problem in determining Δ accurately. Most importantly, the calculation of Δ is based upon determination of d[3,2]. It is quite uncertain how reliable the absolute values of d[3,2] are, since they have been calculated from measurements of volume-averaged particle sizes. Nevertheless, trends in Δ, and the absolute values of reciprocal compressibilities (Δ/d[3,2]), are expected to be accurate.

The ratio of R/Δ is lowered from 30 to about 15 as the polymer molecular weight is increased from 1000 to 34 000, indicating the increased compressibility of the (polymer layer adsorbed on the outside of the) droplets. The cross-linked polymers do not show deviant behavior. It is surprising, however, that this effect of polymer molecular weight on the "compressibility" of the particles is not manifested through a "direct" effect of polymer molecular weight on the adsorbed layer thickness; on the contrary, the high compressibility of droplets coated with high-molecular-weight polymers is mainly due to the small size of the droplets! The observation that an increased polymer molecular weight results in a decrease of lamellar droplet size rather than an increase of the adsorbed layer thickness may be viewed in the same light as the increase of the adsorbed layer thickness observed upon increasing the size of undeformable particles, at constant polymer molecular weight.[12] Both phenomena relate to the strong interdependence of interpolymeric repulsive forces near the particle surface, adsorbed layer thickness [relief of lateral strain through ("longitudinal") extension of the polymer away from the surface], and particle size (relief of lateral strain through increasing the specific surface area).

In light of the above discussion, we propose to generalize the obtained results in the following way:

Low-molecular-weight polymers ($M_w \leq 5300$) are conformationally restricted, and form a relatively thick layer of extended molecules at the surface. The total surface area occupied by the adsorbed polymers (or the lateral

(13) Ploehn, H. J.; Goodwin, J. W. *Faraday Discuss. Chem. Soc.* **1990**, *90*, 77.

(14) (a) Pingret, F. J. V.; Sohm, R. H.; Tadros, Th. F. *Colloids Surf.* **1992**, *65*, 85. (b) Liang, W.; Bagnolo, G.; Tadros, Th. F. *Langmuir* **1995**, *11*, 2899.

(15) We stress that we cannot use any (light scattering) technique which determines the adsorbed layer thickness as the difference in "coated" and "bare" particle size, since the particle size responds to the presence of adsorbed polymer.[3]

(16) Hoffmann, A. C.; Kevelam, J. *AIChE J.* **1999**, *45*, 285.

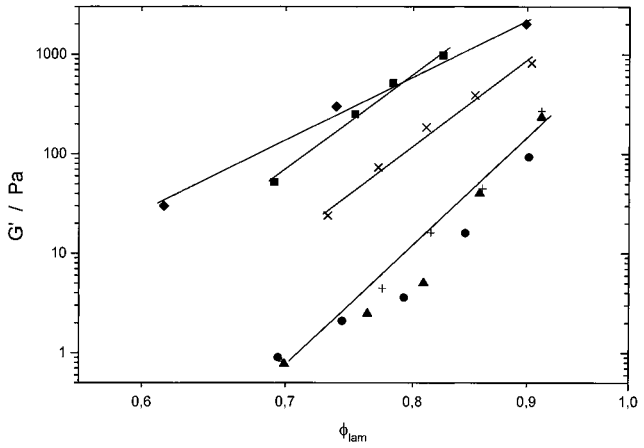

Figure 5. Plots of G' (measured at 1 Hz) vs ϕ_{lam} as a function of molecular weight. ◆ EC34000; ■ EC19000; × EC7800; + RAN4000; ▲ EC3000; ● EC1000.

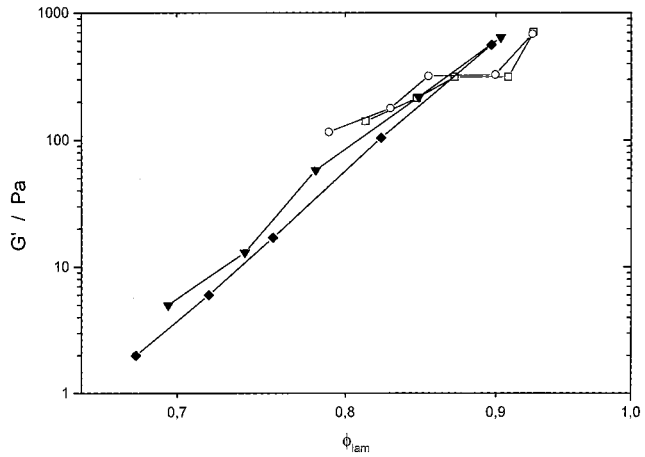

Figure 6. Plots of G' (measured at 1 Hz) vs ϕ_{lam} as a function of the concentration of stabilizing polymer EC7800. □ 1.77 wt %; ○ 1.53 wt %; ▼ 0.34 wt %; ◆ 0.29 wt %.

tension in the adsorbed layer) is relatively low; hence, the average droplet size is large. Thus, both Δ and d[3,2] are relatively high; still, the droplets are characterized by a low compressibility.

High-molecular-weight polymers (M_w > 8000) are conformationally free and adopt a random-coil conformation at the surface of the droplets, such that the stabilizing layer is not greatly radially extended but occupies a large surface area instead. As a result, the adsorbed layer thickness is even smaller than in the case of low-molecular-weight polymers, but the effect of polymer molecular weight on particle size dominates, and the compressibility of the droplets is relatively high.

Elastic Modulus at 1 Hz versus ϕ_{lam}. Figure 5 summarizes the volume fraction dependency of the elastic modulus (at 1 Hz) of lamellar dispersions with added polymers of different molecular weight.

At constant ϕ_{lam}, G' increases with polymer molecular weight. Φ_{lam} is measured as a volume fraction of bare droplets, but the adsorbed polymer layer acts to increase the *effective* volume fraction of the interacting particles. The increasing contribution of the adsorbed polymer layer to the effective volume fraction is (at least partly) responsible for this effect, as appears from the following equation:

$$\phi_{eff} = \phi_{core}\left(1 + \frac{\Delta}{R}\right) \quad (5)$$

It appears that the rheological data can be fitted to the empirical exponential scaling law:

$$G' = k\phi^n \quad (6)$$

Irrespective of polymer molecular weight, the value of the exponent n ≈ 20, which is a typical value for sterically stabilized dispersions, and is indicative of a hard interaction potential. Thus, for R/Δ ratios down to 15, the lamellar droplets show hard-sphere behavior. However, in case of the highest polymer molecular weight, the exponent takes the value of 10. This "soft" interaction potential reflects the large compressibility of the droplets.[17] These results are in full agreement with rheological literature on monodisperse particles.[11,18]

The influence of the concentration of added polymer (EC7800) on the rheological behavior of lamellar droplets is depicted in Figure 6. The curves of elastic modulus versus volume fraction can almost be superimposed in a polymer concentration range of 0.5−1.8 wt % (with respect to a 40/60/20 model system). This seems quite surprising, but it is not: at least in the concentration range of 0.5 < wt % EC7800 < 1, the critical volume fraction is about constant at $\phi_{cr} = 0.7$,[19] and the average droplet size is essentially independent of the amount of added polymer in this concentration range.[4] Thus, the invariance of G' with the amount of added polymer can be explained by the fact that the compressibility of the droplets remains constant. In turn, this is due to the degressive adsorption efficiency with increasing polymer concentration.[4]

Finally, as a general conclusion of the previous sections, many equations and scaling laws that have emerged from rheological studies of monodisperse colloidal particles seem to be successfully applicable to these polydisperse dispersions of lamellar droplets.[20] There is one major difference between the rheology of mono- and polydisperse systems, the latter having much lower absolute values of the moduli at the same volume fraction, but this effect is purely due to differences in packing constraints.[21]

Thickening of and Microstructural Changes in Lamellar Dispersions by Addition of "building-in" Polymers. If the concentration of, for example, EC7800 in a 40/60/20 model lamellar dispersion is increased from 0.1 to 4 wt %, the volume fraction of lamellar droplets will gradually increase from 0.5 to 0.6. (Figure 7). This effect is attributed to the penetration of the (low molecular weight fraction of the) polymers between the lamellar layers, driven by the difference between the polymer concentration in the bulk solution (continuous phase) and in the hydration layers of the lamellar droplet. At the outset, we expect that building-in not only depends on the polymer concentration (difference) but also on the structure of the polymer: the lower its molecular weight, the smaller its hydrodynamic radius and the better it fits between the lamellar layers. Indeed, the increase of ϕ_{lam}

(17) Mewis, J.; Frith, W. J.; Strivens, T. A.; Russel, W. B. *AIChE J.* **1989**, *35*, 415.

(18) Tadros, Th. F.; Liang, W.; Costello, B.; Luckham, P. F. *Colloids Surf. A* **1993**, *79*, 105.

(19) In case of higher polymer concentrations, plots of G''/G' vs ϕ are ill-behaved for unknown reasons.

(20) We note one important exception. When applying the Krieger−Dougherty equation to polydisperse systems, the large value of $\phi_{eff,\ max}$ that one will find cannot be (purely) attributed to "soft" adsorbed layers, as is often done in studies of colloidal suspensions of monodisperse particles, but is mainly due to polydispersity effects. See: Mewis, J.; D'Haene, P. *Makromol. Chem., Macromol. Symp.* **1993**, *68*, 213.

(21) Richtering, W.; Müller, H. *Langmuir* **1995**, *11*, 3699.

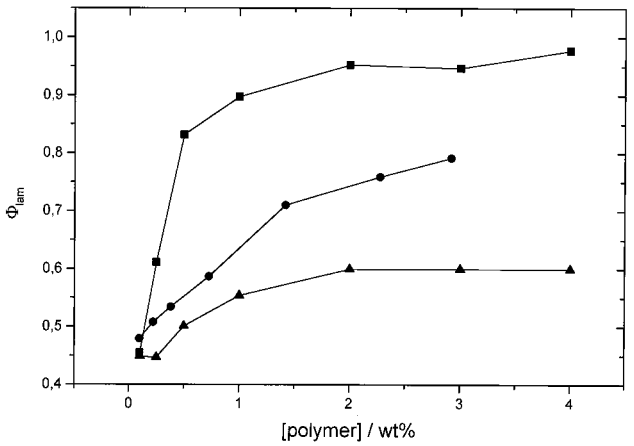

Figure 7. Plots of ϕ_{lam} vs polymer concentration, for different polymer molecular weights. ■ EC750; ● FEC3000; ▲ EC7800.

with polymer concentration is more pronounced the lower the polymer molecular weight (Figure 7). Moreover, it is expected that the occurrence of building-in is accompanied by an increase of the lamellar repeat distance. X-ray diffraction measurements unequivocally demonstrate the process of building-in: the lamellar repeat distance increases from 3.54 (0.1 wt % EC750) to 3.71 (1 wt % EC750) to 7.07 nm (4 wt % EC750).

The microstructure of a 40/60/20 model system with various amounts of added building-in polymer EC750 has been investigated in more detail by visual observation and light and freeze-fracture electron microscopy. As more and more polymer is added to the 40/60/20 model system, the appearance of the "dense white"[22] lamellar dispersion is changed dramatically to a semitransparent gel-like substance. These observations lead us to believe[23] that the lamellar dispersion gradually makes place for a continuous lamellar phase. Indeed, light microscopy indicates that at the highest concentration of EC750 most droplets have disappeared, while some optically birefringent striations emerge, which indicate the presence of a continuous lamellar phase (Figure 8c).[24]

Electron microscopy supports these statements. In case of dispersions containing 0.1 wt % of EC750, mainly surface-fractured, discrete spheres are observed (Figure 8a). The fracturing of the spheres over their surface hints at appreciable differences between the intralamellar forces and the interactions between the droplets and their surroundings (i.e., neighboring droplets or continuous phase).[25−27] Thus, at small polymer concentrations, the sample appears to possess an inhomogeneous structure in which lamellar droplets are observed as discrete entities. In contrast, in the presence of 4 wt % of EC750, the sample is mainly cross-fractured (Figure 8c). The volume fraction of the lamellar phase is almost unity, and cross-fracturing therefore indicates small interaction differences between intra- and interlamellar forces. The sample is relatively homogeneous, suggesting a "continuous" lamellar structure. Herein, "continuous" refers to a lamellar morphology coexisting of planar structures and spherical units,[28] which is in line with current viewpoints.[29]

The transition of a lamellar dispersion to more continuous structures is rationalized as follows. Lamellar droplets are characterized by a nonzero spontaneous curvature. This is due not only to an asymmetric distribution of surfactant molecules in the bilayers, but also to the presence of the adsorbed polymer layer.[3] However, as the polymers penetrate the lamellar droplets, both inter- and intralamellar steric repulsion forces are introduced. As ϕ_{lam} approaches unity, the system appears to minimize the total repulsion energy by transforming the curved droplets into continuous lamellar structures, for which the magnitudes of the intra- and interlamellar repulsive forces are equal.

The rheological properties of lamellar dispersions with building-in polymers are *intrinsically* not very different from those of sterically stabilized dispersions with higher molecular weight polymers. $G'(\phi)$ for a dispersion containing 0.1 wt % or 1 wt % of EC750 (EC750k1 or EC750k6; Figure 9) is lowest for all of the samples that have been investigated, and this is due to a marginal contribution of the adsorbed layer thickness to the effective volume fraction, as discussed above.

Of course, if plotted against nominal surfactant concentration, the elastic modulus of lamellar dispersions with added building-in polymers greatly exceeds G' of dispersions containing polymers that remain exclusively at the droplet surface. Thus, low-molecular-weight stabilizing polymers can be used to thicken lamellar dispersions (at constant surfactant concentration).

Thickening of Lamellar Dispersions by Addition of Bridging Polymers. At the outset, we expect that polymers bearing multiple anchoring groups strengthen the network of lamellar droplets by forming bridges between neighboring particles. Two different bridging polymers have been designed. The first type was obtained by chemical cross-linking of endcapped stabilizing polymers, designated as CL3500 and CL9000. Indeed, these polymers appear to enhance the elastic modulus (at constant ϕ_{lam}); see Figure 10. Since the droplets are not flocculated (Figure 11), the bridging interactions are weak. In contrast, a random copolymer of sodium acrylate and lauryl methacrylate, containing ca. 10 anchors per molecule, is a much more effective bridging agent. $G'(\phi)$ for HMNAR exceeds the elastic moduli of all dispersions that have been investigated (Figure 10). In this particular case, the mechanism is bridging flocculation as appears from Figure 12B. We note that the flocculation of the droplets is reversible: if EC7800 is admixed in equal proportions, the droplets are redispersed (light micrographs not shown).

This observation of reversible flocculation led us to investigate 40/60/20 model lamellar dispersions containing equal (weight) amounts of bridging polymer and hydrophobically endcapped polymer, using shear viscosimetry. It was anticipated that the lamellar dispersions might show shear-thinning behavior: at low shear stresses, the droplets are involved in a network held together by bridging polymers; however, if more shear is applied, e.g., by "pouring", the network breaks down and the dispersion is able to flow. Thus, the viscosity of the sample should drop with increasing shear. As appears from Figure 13, addition of 1 wt % of a bridging polymer to a lamellar dispersion containing 1 wt % of EC7800 indeed greatly enhances the viscosity of the sample at low shear rates,

(22) Forge, A.; Lydon, J. E.; Tiddy, G. J. T. *J. Colloid Interface. Sci.* **1977**, *59*, 186.
(23) Winsor, P. A. In *Liquid Crystals and Plastic Crystals*; Gray, G. W., Winsor, P. A., Eds.; Ellis Horwood: Chichester, U.K., 1974; Vol. 1.
(24) Hartshorne, N. H. *The Microscopy of Liquid Crystals*; Microscope Publications: London, 1974.
(25) Simonds, D. H. *Baker's Dig.* **1974**, *48*, 16.
(26) Buchheim, W. *Food Microstruct.* **1982**, *1*, 189.
(27) Heertje, I. *Food Struct.* **1993**, *12*, 77.
(28) James, C. J.; Heathcock, J. F. *J. Chem. Soc., Faraday Trans. 1* **1982**, *77*, 2857.
(29) (a) Fifield, R. *New Sci.* **1980**, *88*, 150. (b) Pas, J. C., van de, *Ph.D. Thesis*; University of Groningen: Groningen, The Netherlands, 1993; p 36.

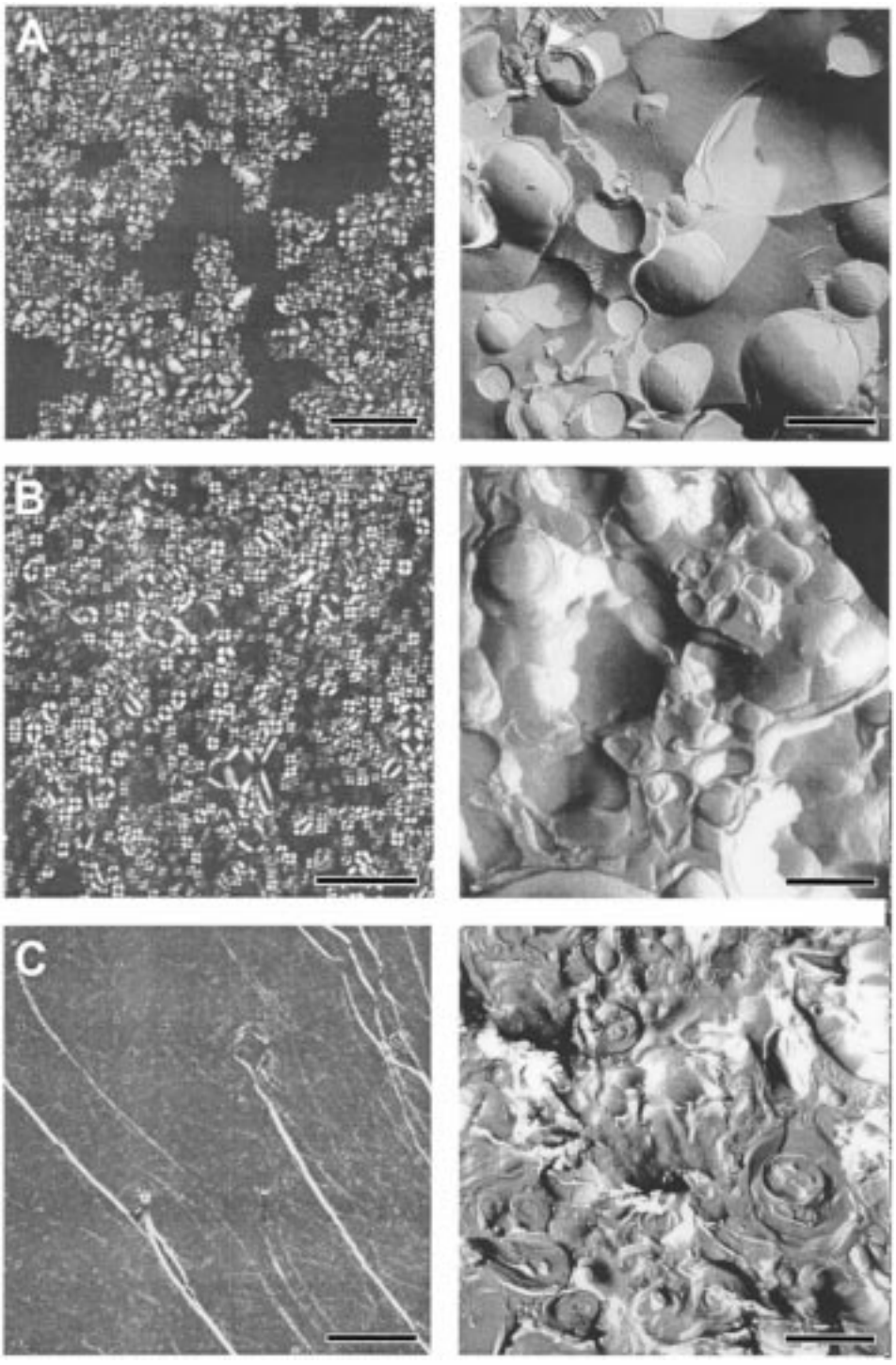

Figure 8. Polarized light micrographs (left) and freeze-fracture electron micrographs (right) of 40/60/20 lamellar dispersions containing different concentrations of EC750. A: 0.1 wt % of EC750. Bar represents 25 μm (LM), 3 μm (FFEM). B: 1 wt % of EC750. Bar represents 25 μm (LM), 0.5 μm (FFEM). C: 4 wt % of EC750. Bar represents 100 μm (LM), 1 μm (FFEM).

whereas the viscosities at higher shear rates (corresponding to "pouring" conditions, 21 s^{-1}) are very similar for samples with or without added bridging polymers. This means that a dispersion of lamellar droplets containing both stabilizing and bridging polymers is capable of suspending solid particles, and can be easily poured at the same time.

Rheological Behavior and Interaction Potential: A Closer Look at Steric Stabilization. It has been established by various authors, using optical diffraction and other techniques,[30] that latex particles can form an ordered array with the particles sited on a time-averaged basis at points on a lattice. Under these conditions, characterized by high volume fractions of particles, the equilibrium array of particles is disturbed by an oscillatory shear. If the time period of the wave is small compared with the relaxation time of the particles in the array, then the elastic modulus is related from the restoring force driving the particles to their equilibrium positions in the repulsive network. Buscall et al.[3] derived a general equation relating the theoretical shear (or high-frequency

(30) (a) Goodwin, J. W.; Ottewill, R. H.; Parentich, A. *J. Phys. Chem.* **1980**, *84*, 1580. (b) Hachisu, S.; Kobayashi, Y.; Kose, A. *J. Colloid Interface Sci.* **1973**, *42*, 342.

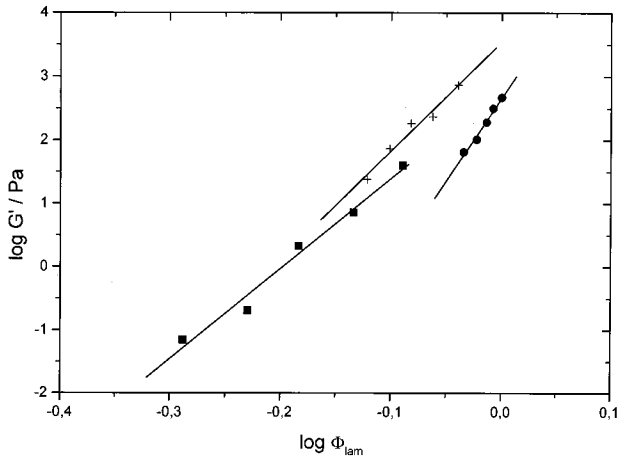

Figure 9. Plots of $G'(\phi)$ showing the influence of building in on the rheological properties of 40/60/20-type lamellar dispersions. + 1 wt % of EC7800; ■ 0.1 wt % of EC750; ● 1 wt % of EC750.

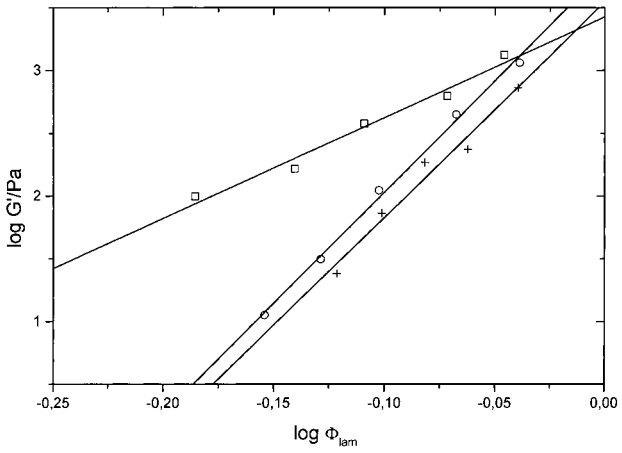

Figure 10. Plots of $G'(\phi)$ showing the influence of bridging polymers on the rheological properties of 40/60/20-type lamellar dispersions. □ 1 wt % of HMNAR; ○ 1.15 wt % of CL9000; + 1 wt % of EC7800.

elastic) modulus (G_{th}) to the interparticle potential energy dependence of the particle separation [$V(h)$]:

$$G_{th} = \frac{\gamma}{h_c} \cdot \frac{\partial^2 V(h_c)}{\partial h_c^2} \tag{7}$$

Herein, γ is a geometrical factor, corresponding to $^3/_{32} \times \phi_{max} \times m$. For face-centered cubic structures, the coordination number $m = 12$; in case of a body-centered cubic array, $m = 8$. For the lamellar dispersions under study, the exact value of γ is unknown; however, we do not make a large error if we assume that $\phi_{max} = 1$ and $\gamma = 1$. h_c is the center-to-center interparticle distance, which is written as:

$$h_c = 2R\left(\frac{\phi_{max}}{\phi}\right)^{1/3} \tag{8}$$

This approach can be used to fit an interparticle potential theoretically derived for sterically stabilized dispersions to the experimentally determined dependence of the elastic modulus on the interparticle distance. For example, Howe et al. proposed that the potential energy of sterically stabilized particles scales with the ratio of the adsorbed layer thickness (Δ) to the surface-to-surface particle separation (h):[31]

$$V(h) \propto \frac{\Delta}{h} \tag{9}$$

The surface-to-surface particle separation differs from the center-to-center distance by twice the radius of the particle:

$$h = h_c - 2R \tag{10}$$

Since the particle radius is virtually independent of either h or h_c, we may write

$$\frac{\partial^2 V(h_c)}{\partial h_c^2} = \frac{\partial^2 V(h_c)}{\partial h^2} \tag{11}$$

Hence, the elastic modulus is predicted to scale with the surface-to-surface interparticle separation according to

$$G_{th} \propto \frac{1}{h_c}\frac{\Delta}{h^3} = \frac{\Delta}{h^4 + 2Rh^3} \approx \frac{\Delta}{2Rh^3} \; (R \gg h) \tag{12}$$

Therefore, a plot of log G' versus log h should yield a straight line with a slope of -3. This prediction compares rather well with the results obtained from a log−log plot of $G'(h)$ for lamellar dispersions containing endcapped polymers with a molecular weight ranging between 1000 and 19 000. As appears from Figure 14, the correlation is not very good, but it is linear, with a slope of -3.4. The large scattering of the data is related to the fact that the particle radii and adsorbed layer thicknesses are not truly constant (i.e., they are dependent on the molecular weight of the polymer). Still, these approximate calculations allow us to understand qualitatively the rheological behavior of lamellar dispersions with added hydrophobically endcapped polymers.

A more sophisticated approach was taken by Zhulina et al.[32] These authors describe the interparticle potential of sterically stabilized particles in terms of a self-consistent field model, taking quantitatively into account the parameters characterizing solvent quality, and conformational Gibbs energy of the adsorbed polymer. For compressed layers, they predict the following interparticle potential:

$$V(q) = \frac{f\Delta G_p^0}{2\omega}\left(\frac{\pi^2}{12\alpha q} - \pi\beta \ln q + \text{const.}\right) \tag{13}$$

where $q = h/\Delta$, $\omega = R/\Delta$, f is the number of polymers adsorbed on each droplet, and ΔG_p^0 is the conformational Gibbs energy per anchored polymer. α and β are dimensionless constants related to the chain expansion and flexibility; for a good solvent, $\alpha \approx 1$ and $\beta \approx 1$.[33] An important and realistic assumption is that $R \gg \Delta$. Moreover, the polymers are assumed to be adsorbed as brushes (the lateral tension in the adsorbed layer is large).

(31) Howe, A. M.; Clarke, A.; Whitesides, T. H. *Langmuir* **1997**, *13*, 2617.

(32) Zhulina, E. B.; Borisov, O. V.; Priamitsyn, V. A. *J. Colloid Interface Sci.* **1990**, *137*, 495.

(33) Unfortunately, the authors do not explicitly define these parameters.

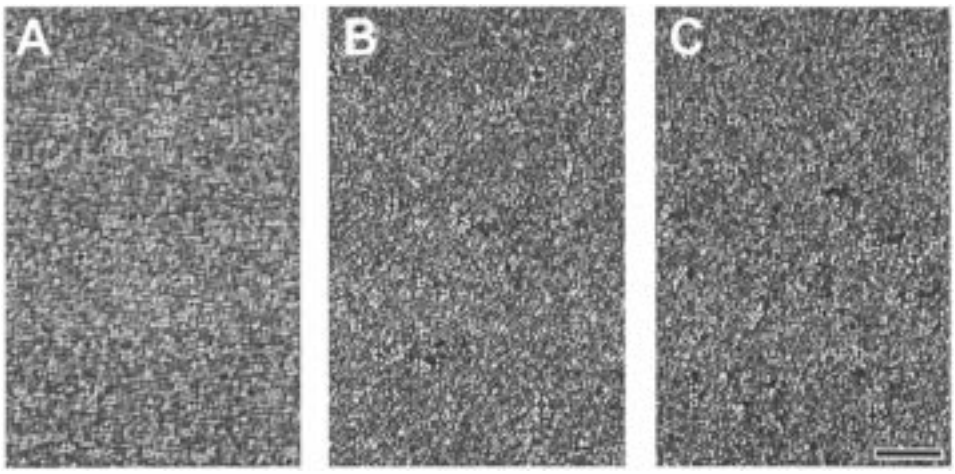

Figure 11. Polarized light micrographs of concentrated 40/60/20-type lamellar dispersions ($\phi_{lam} \approx 0.75$) containing 1 wt % of EC7800 (A), 0.45 wt % of CL3500 (B) and 1.15 wt % of CL9000 (C). Bar represents 100 μm. Note that all samples are deflocculated.

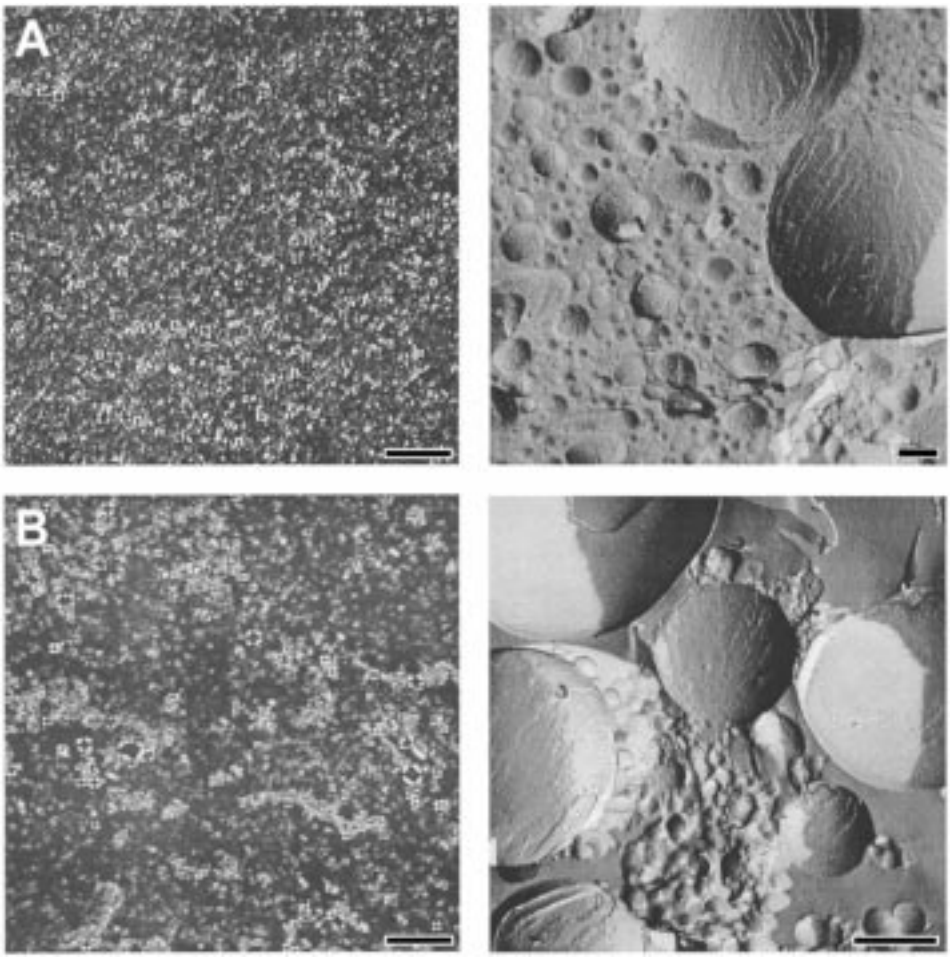

Figure 12. Polarized light micrographs (left) and freeze-fracture electron micrographs (right) of 40/60/20 dispersions containing 2 wt % of EC7800 (A) and 2.5 wt % of HMNAR (B). The sample containing HMNAR is flocculated, the dispersion containing EC7800 is deflocculated. Bars represent 100 μm (light micrographs) or 1 μm (FFEM).

This was shown to be the case for the lamellar dispersions under study.[4]

Substitution of eq 13 into eq 7 yields an expression for the theoretical elastic modulus of sterically stabilized dispersions as a function of interparticle separation:

$$G_{th} = \frac{\gamma f \Delta G_p^0}{2\omega h_c}\left(\frac{\pi^2 \Delta}{6\alpha h^3} + \frac{\pi\beta}{h^2}\right) \qquad (14)$$

We note that the right-hand side of the expression has the right units. Finally, we express the elastic modulus in terms of a volume fraction dependence (assuming that $\phi_{max} = 1$):

$$G_{th} = \frac{\gamma f \Delta G_p^0}{16\omega R \phi^{-1/3}}\left(\frac{\pi^2}{12\omega\alpha R^2[\phi^{-1/3} - 1]^3} + \frac{\pi\beta}{R^2[\phi^{-1/3} - 1]^2}\right) \qquad (15)$$

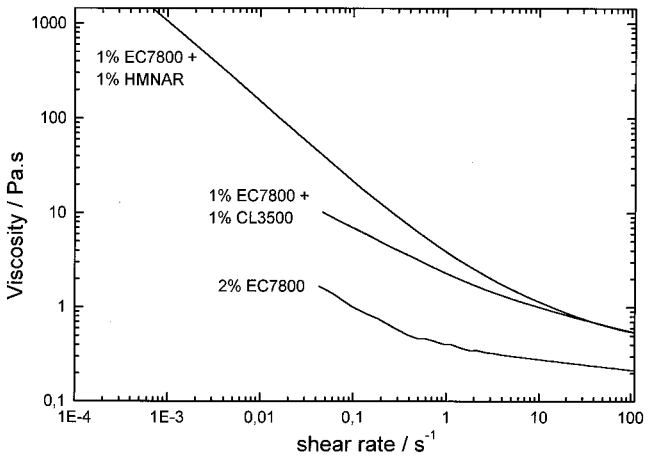

Figure 13. Viscosities of sterically stabilized 40/60/20 lamellar dispersions with added bridging polymers as a function of shear rate.

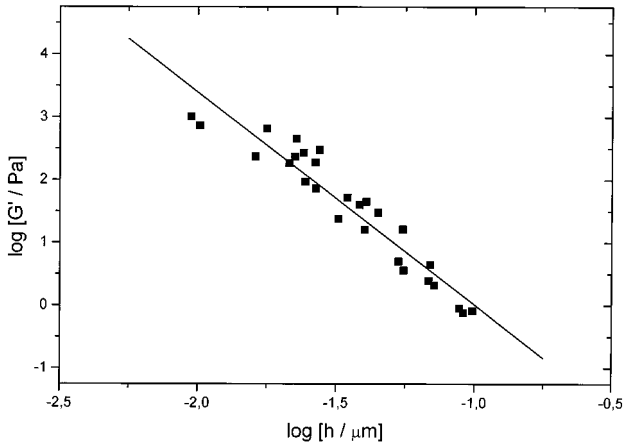

Figure 14. Log−log plots representing the dependence of elastic modulus (G') on surface-to-surface interparticle separation (h) for lamellar dispersions with added hydrophobically endcapped poly(sodium acrylate)s.

Rearrangement yields the following expression:

$$G_{\mathrm{th}} = \frac{\gamma f \Delta G_{\mathrm{p}}^{0}}{16\omega R^{3}} \frac{\phi^{1/3}}{(\phi^{-1/3}-1)^{2}}\left(\frac{\pi^{2}}{12\omega\alpha(\phi^{-1/3}-1)} + \pi\beta\right) \quad (16)$$

The next step is to relate the experimentally determined elastic modulus to the volume fraction of lamellar droplets, through eq 16, in a nonlinear fit procedure. The values of α, β, and γ have been fixed at 1, which is a reasonable approximation (vide supra). In any case, these parameters are expected to be approximately constant among the series of endcapped poly(sodium acrylate)s under study, and fixing their values makes the fit procedure statistically more reliable. Likewise, R and ω were not allowed to vary in the fit procedure. These parameters were fixed at the values that were experimentally obtained for each specific combination of lamellar dispersion and endcapped poly(sodium acrylate). The particle radius (R) was identified with d[3,2]. Thus, the product $f\Delta G_{\mathrm{p}}^{0}$, which is the conformational Gibbs energy of the polymer layer adsorbed on a lamellar droplet, is left as the only variable fit parameter. The results obtained are shown in Figure 15.

Equation 16 describes the experimental data surprisingly well, in view of the fact that only one fit parameter has been used. The dependence of the conformational Gibbs energy of the adsorbed polymer layer on polymer molecular weight does not follow a clear trend; $f\Delta G_{\mathrm{p}}^{0} =$ 1 ± 0.5 kJ for all polymers under study.[34] This result is not unexpected, since the conformational Gibbs energy per polymer ($\Delta G_{\mathrm{p}}^{0}$) is inversely related to the number of polymer molecules adsorbed per droplet (f) through the lateral pressure in the adsorbed polymer layer. Thus, the surfaces of large droplets are occupied by relatively large numbers of low-molecular-weight polymers that do not strongly repel each other: f is large and $\Delta G_{\mathrm{p}}^{0}$ is small. On the other hand, at constant hydrophobic anchor density, replacing the low-molecular-weight polymers by high-molecular-weight analogues increases the lateral repulsion between adsorbed polymer molecules. The large droplets react by reducing their size and forming a larger number of smaller particles (this is an experimental fact; cf. Table 2). Hence, f is reduced. Despite the fact that the total surface area available to the polymer molecules has been enlarged, $\Delta G_{\mathrm{p}}^{0}$ is still larger than the conformational Gibbs energy of low-molecular-weight polymers since the interfacial (and curvature) Gibbs energy of the droplets has been raised.

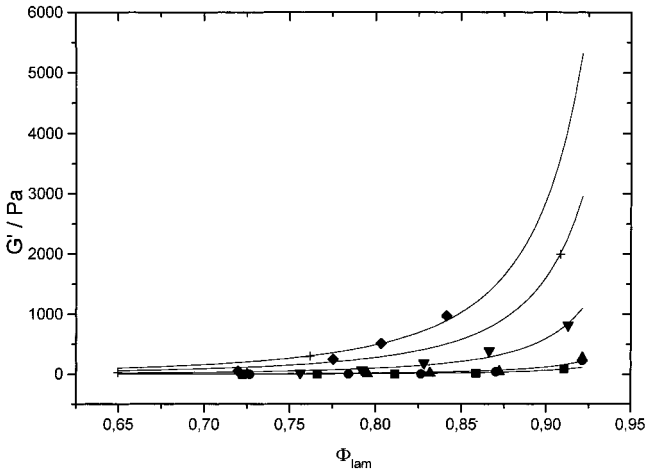

Figure 15. Plots of G' vs Φ_{lam} for lamellar dispersions containing endcapped polymers of different molecular weights. The lines represent fits of the data to eq 16. + EC34000; ◆ EC19000; ▼ EC7800; ▲ RAN4000; ● EC3000; ■ EC1000.

In conclusion, we can describe the elastic modulus of concentrated lamellar dispersions with added hydrophobically endcapped poly(sodium acrylate)s in terms of an interparticle potential energy corresponding to sterically stabilized particles. We learn from the fit analysis that the conformational Gibbs energy of the adsorbed polymer layer, which determines the equilibrium droplet size, is rather invariant with polymer molecular weight.

Conclusions

The rheological behavior of dispersions of sterically stabilized polydisperse lamellar droplets can be described using empirical scaling models that have been developed for colloidal suspensions of monodisperse particles. Elastic moduli are exponentially dependent on ϕ_{lam}, and the large value of the exponent, which is independent of polymer molecular weight up to at least 19 000, indicates that the lamellar droplets behave as hard spheres down to a R/Δ ratio of 15. At constant core volume fraction, the elastic modulus increases with the molecular weight of the adsorbed polymer due to the increase of the effective volume fraction. $G'(\phi)$ hardly depends on the amount of polymer added due to the fact that the compressibility of the droplets is rather insensitive to the polymer concentration. Plots of log G' versus log h are linear and can be

(34) Individual errors in f $\Delta G_{\mathrm{p}}^{0}$ amount to 5−10%.

fitted successfully to and understood in terms of models describing the interparticle potential as logarithmic or hyperbolic functions of interparticle distance.

Interestingly, theoretical models relating the elastic modulus of concentrated (lamellar) dispersions to an interparticle pair potential corresponding to sterically stabilized droplets are quite successful to describe the experimentally determined dependence of the volume fraction of lamellar droplets on G'.

Cross-linking of the stabilizing polymers is an effective means of thickening the dispersion. In addition, colloidal dispersions of lamellar droplets can be thickened by the addition of low-molecular-weight hydrophobically end-capped poly(sodium acrylate)s. These molecules penetrate into the droplets, thereby increasing the water layer thickness and, consequently, ϕ_{lam}. Optimal shear-thinning properties are obtained by adding high-molecular-weight random copolymers of sodium acrylate and lauryl methacrylate to sterically stabilized lamellar dispersions.

Acknowledgment. We gratefully thank W.M. du Chatinier for determining the molecular weights of the polymers and Drs. M. Paques, M. Leunis, and R. den Adel for recording all freeze-fracture−etching electron micrographs. Dr. Niek Buurma kindly assisted in performing the tedious algebra. Discussions with Prof. J. Mellema on the rheological behavior of dispersions are gratefully acknowledged.

LA9816353